福井大学
工学部 研究報告
第36巻 第1号
昭和63年3月

Modeling and Control of a Double-Walled Thermostatic Container

Toshiyuki ASAKURA*, Hiroo UCHIYAMA** and Masaru DANNO*

(Received Feb.10, 1988)

This research is concerned with the modeling and control of a double-walled thermostatic container. This container is an important element of a device which measures the difference of pressures between two points in tunnels. The principle of this measuring method is comparison between constant pressure in the container and external one at two points.(1) In order to obtain the exact constant pressure, the temperature in the container must be controlled at a high accuracy within 10^{-3}°C. In this paper, analytical and experimental studies are developed for both modeling and control of temperature dynamics in the container.

First, several parameters of a bilinear control system can be estimated using the least-squares and the correlation -regression algorithms from input-output measurements. Using these parameters, the temperature in the container can be estimated. Next, the ambient air temperature influences the accuracy of the temperature control in the container. In order to eliminate this influence , a feedforward controller is added to regulate the output of the heater according to the atmospheric temperature. The experimental results show the good regulation.

I. Introduction

This paper develops both the estimation of the controlled temperature and the control strategy to keep at a constant temperature with high accuracy for a double-walled thermostatic container,

* Dept. of Mech. Engi., ** Matsushita Communication Co. Ltd.

which is one of the most important elements in the measuring device of the barometric differences.[1][2] Now, if we demand the accuracy within ±0.2Pa on the measuring device, it is necessary for the container to be kept at a constant temperature with the accuracy of 10^{-3}°C. For this purpose, we already proposed a thermostatic device which consists of the double-walled container. In this device, the space between the inner and outer casings, which is called as the intermediate space, can be thermostated at 50°C by the on-off regulation of the heater. At a result, the air temperature in the inner container, which is called as the inner space, can be kept constant with high accuracy of 10^{-3}°C.

In the research on the trial device already implemented,[2] each parameter values for the inner and outer containers have been determined through the transient response experiments, from which the theoretical analysis has been performed with respect to the variation of the temperature in the intermediate space. However, these experiments require much trouble and also there exists a fairly difference between theoretical and experimental values.

In this paper, a parameter estimation method is presented which determines the parameters for both the inner and outer containers using all informations contained in the input and output data of the temperature control system. Based on the estimated parameters, the states of the temperature in the intermediate and inner spaces can be estimated precisely.

Next, one of the problems is that the thermostatic container is always subjected to the effect of the ambient temperature. That is, due to the fluctuation of the ambient temperature, the center position of temperature oscillation in the intermediate space changes in the steady-state. Then, the temperature characteristics in the inner space suffers a harmful influence. In order to avoid this unfavorable effect, the feedforward controller is equipped with this thermostatic control system to regulate the output of the heater according to the variation of the atmospheric temperature. From the experimental results, it is seen that the variation of the steady-state oscillation due to the effect of the ambient temperature can be taken away and also a favorable thermostatic characteristics can be obtained.

2. Structure of Thermostated Device and Block Diagram

2.1 Structure The structure of thermostated device is shown in Fig.1, which consists of a double-walled container. The outer

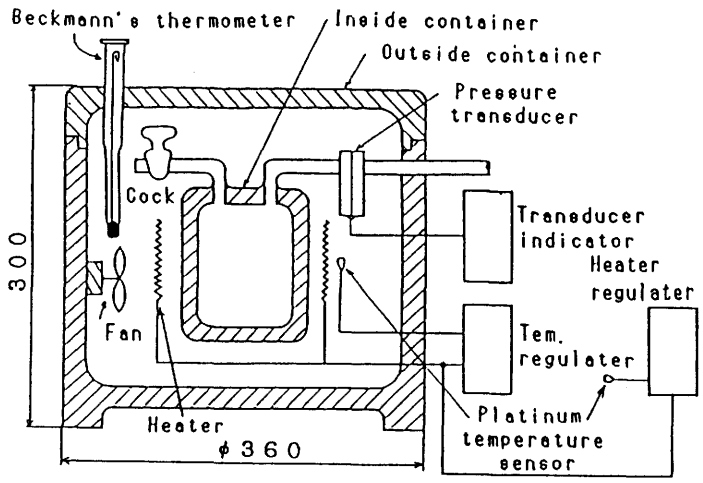

Fig.1 Structure of a Double-Walled Thermostatic Device

casing is made of the stylene form and the inner one the special glass covered by the stylene form. The intermediate space between two casings can be thermostated at 50°C by the on-off regulation of the heater. From this regulation and heat transfer characteristics of the inner vessel, the inner space can be structurally kept at a constant temperature with higher accuracy, comparing with the intermediate space. In the intermediate space, the small fan to uniform the temperature in the space, thermometer and the pressure transducer to detect the difference of the pressure between the ambient air and the one in the inner space are settled. Furthermore, in order to eliminate the effect of the ambient temperature for ones both in the intermediate and inner spaces, the output of the heater can be precisely controlled through the detection of the ambient temperature by the use of a platinum temperature sensor.

2.2 **Block diagram** The principal symbols are denoted as follows;

c_1, c_0 ; heat capacities of inner and intermediate spaces

σ_1, σ_0 ; heat transfer coefficients of outside and inside containers

G_1, G_0 ; transfer functions of inner and intermediate spaces

$\Delta\theta_1, \Delta\theta_0$; difference of temperature from the reference states in the inner and intermediate spaces

Δq ; total heating value generated from electric heater and fan etc.

The transfer functions $G_0(s)$ of the intermediate space and $G_1(s)$ of the inner space are represented by [2]

$$G_0 = \frac{c_1 s+\sigma_1}{c_0 c_1 s^2+(c_0\sigma_1+c_1\sigma_1+c_1\sigma_0)s+\sigma_0\sigma_1} \tag{1}$$

and

$$G_1 = \frac{1}{1+(c_1/\sigma_1)s} . \tag{2}$$

Also, the transfer function $G_s(s)$ of the sensor is given by

$$G_s(s) = \frac{K_s}{1+T_s s} , \tag{3}$$

where K_s is a temperature coefficient of the sensor and T_s a time constant of the sensor.

Letting the desired temperature (50°C) as the reference state, the relay element in the case of θ_{as}=7.9°C where θ_{as} presents the reference ambient temperature of this device is shown as Fig.2(a). For the relay element in Fig.2, let 2h be a hysterisis width, Z an input amplitude and 2A an output magnitude where A=11.1w. If the atmospheric temperature rises $\Delta\theta_a$ more than θ_{as}, it can be considered that the relay element becomes non-symmetric as shown in Fig.2(b). As a result, the center position of the steady-state oscillation of the temperature in the intermediate space shows a rizing trend and then the accuracy becomes worse. In order to eliminate the effect due to the variation of the atmospheric temperature, it is necessary to reduce the output of the heater only by $2\sigma_0\Delta\theta_a$, as shown by the broken line in Fig.2(b). For this purpose, the feedforward controller may be supplemented to regulate the output of the heater by the previous detection of the atmospheric temperature. Figure 3 represents the block diagram with respect to the thermostatic device with the feedforward controller, which is shown in Fig.1.

For the convenience of analysis, the simplified block diagram is shown in Fig.4. In Fig.4, $\gamma(t)$ is a random noise which generates mainly through the stirring of the air due to the fan in the intermediate space. Also, K is the gain constant of the amplifier.

3. Parameter Estimation

Using Eq.(1), the dynamic model representing the relation between $\Delta\theta_0$ and Δq may be written by the following differential equation,

$$\frac{d^2\Delta\theta_0}{dt^2}+\left(\frac{\sigma_1}{c_1}+\frac{\sigma_1}{c_0}+\frac{\sigma_0}{c_0}\right)\frac{d\Delta\theta_0}{dt}+\frac{\sigma_1\sigma_0}{c_1c_0}\Delta\theta_0-\frac{1}{c_0}\left(\frac{d\Delta q}{dt}+\frac{\sigma_1}{c_1}\Delta q\right)=\kappa w . \tag{4}$$

Here, it is assumed that $w(t)$ is a white Gaussian noise with

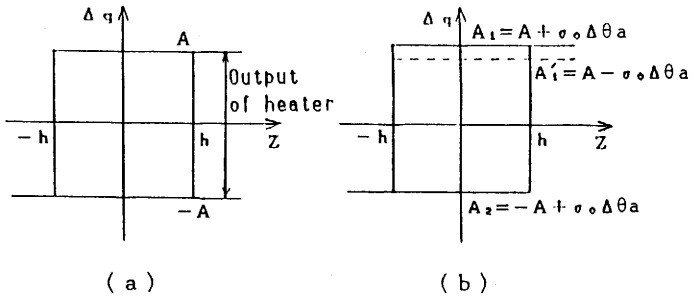

Fig.2 The Characteristics of Relay Element

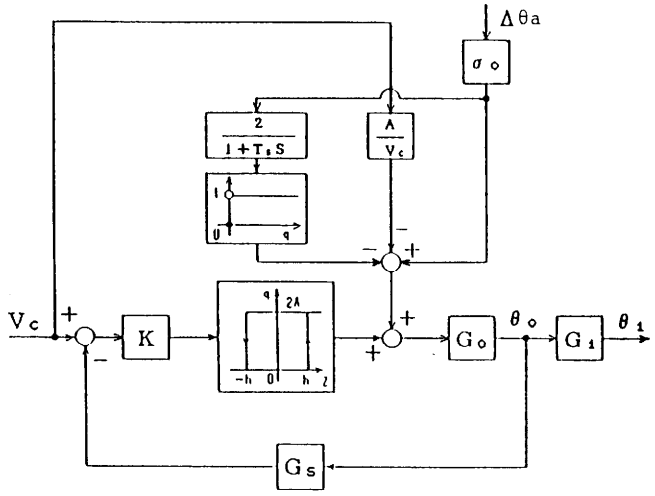

Fig.3 Block Diagram of Thermostatic Device with Feedforward Controller

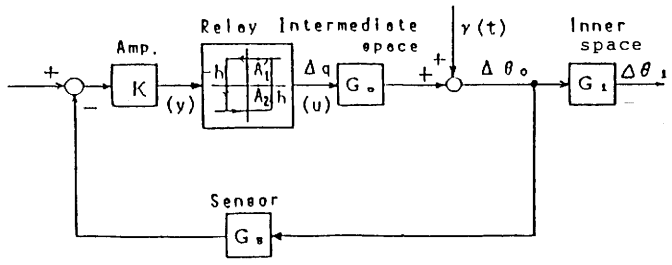

Fig.4 Simplified Block Diagram

zero mean, which is made of $\gamma(t)$. Define the state variables by

$$\Delta\theta_0 = x_1, \quad \frac{d\Delta\theta_0}{dt} - \frac{1}{c_0}\Delta q = x_2, \quad \Delta q = u.$$

The equation (4) is rewritten by the state equation,

$$\frac{d}{dt}\begin{bmatrix} x_1 \\ x_2 \end{bmatrix} = \begin{bmatrix} a_{11} & a_{12} \\ a_{21} & a_{22} \end{bmatrix}\begin{bmatrix} x_1 \\ x_2 \end{bmatrix} + \begin{bmatrix} k_1 \\ k_2 \end{bmatrix} u + \begin{bmatrix} d_1 \\ d_2 \end{bmatrix} w \ , \tag{5}$$

where the model parameters are given by $a_{11}=0$; $a_{12}=1$; $a_{21}=-\sigma_1\sigma_0/(c_1c_0)$; $a_{22}=-(\sigma_1/c_1+\sigma_1/c_0+\sigma_0/c_0)/c_0$; $k_1=1/c_0$; $k_2=\sigma_1/(c_1c_0)-(\sigma_1/c_1+\sigma_1/c_0+\sigma_0/c_0)/c_0$; $d_1=0$; $d_2=\kappa$, and σ is a constant.

To estimate the unknown system parameters from the input-output measurements, the input-output relation is presented in the following. Let ΔT be the discretizing interval. The system model (5) can be represented by a discrete-time state variable model,

$$x(k+1) = \begin{bmatrix} \phi_{11} & \phi_{12} \\ \phi_{21} & \phi_{22} \end{bmatrix} x(k) + \begin{bmatrix} D_1 \\ D_2 \end{bmatrix} u(k) + \begin{bmatrix} F_1 \\ F_2 \end{bmatrix} w(k), \tag{6}$$

where $\phi_{11}=(\lambda_1 e^{\lambda_2\Delta T}-\lambda_2 e^{\lambda_1\Delta T})/(\lambda_1-\lambda_2)$; $\phi_{12}=(e^{\lambda_1\Delta T}-e^{\lambda_2\Delta T})/(\lambda_1-\lambda_2)$; $\phi_{21}=\lambda_1\lambda_2(e^{\lambda_2\Delta T}-e^{\lambda_1\Delta T})/(\lambda_1-\lambda_2)$; $\phi_{22}=(\lambda_1 e^{\lambda_1\Delta T}-\lambda_2 e^{\lambda_2\Delta T})/(\lambda_1-\lambda_2)$; $D_1=[k_1\{(\lambda_1+\lambda_2)(\phi_{11}-1)-\phi_{21}\}-k_2(\phi_{11}+1)]/(\lambda_1\lambda_2)$; $D_2=k_1(\phi_{11}-1)+k_2\phi_{12}$; $F_1=-\kappa(\phi_{11}+1)/(\lambda_1\lambda_2)$; $F_2=\kappa\phi_{12}$, and where $\lambda_1,\lambda_2=a_{22}/2\pm\sqrt{a_{22}^2+4a_{21}}/2$.

Letting the transfer function of the temperature sensor be expressed by time delay element e^{-Ls}, and also μ an integral number of the value $L/\Delta T$, then the output $y(k)$ is given by

$$y(k) = [G \ 0]\, x(k-\mu) + v(k), \tag{7}$$

where G is the gain constant as

$$G = KK_s/\sqrt{1+T_s^2(2\pi/T)^2}. \tag{8}$$

Here, T is the period of the temperature oscillation in the intermediate space. Also, $v(k)$ in Eq.(7) represents the observation noise, which is a zero mean white Gaussian random sequence. The input signal $u(k)$ to the intermediate space is assumed to be uncorrelated with both $w(k)$ and $v(k)$.

Equations (6) and (7) yield the input-output model (Appendix A)

$$\begin{aligned} y(K+2) = {} & a_2 y(k+1) + a_1 y(k) + b_2 u(k+1-\mu) \\ & + b_1 u(k-\mu) + \xi(k+2), \end{aligned} \tag{9}$$

where $a_2=\phi_{11}+\phi_{22}$; $a_1=\phi_{12}\phi_{21}-\phi_{11}\phi_{22}$; $b_2=GD_1$ and $b_1=G(\phi_{12}D_2-\phi_{22}D_1)$. $\xi(k+2)$ is a composite noise term containing both the state noise and the measurement one.

The unknown system parameters a_1, a_2, b_1 and b_2 in Eq.(9) are estimated based on both the experimental data u(t) and y(t), in which u(t) is the input signal with a periodic pseudorandom binary sequence and y(t) the output signal representing the sample behavior of the temperature variation in the intermediate space. The least-squares algorithm and the correlation-regression algorithm are used to estimate the unknown parameters.[3][4] Now, the correlation functions with limit in the mean-square sense are defined as

$$\begin{aligned}\psi_{yu}(j) &= \lim_{N\to\infty}\frac{1}{N}\sum_{k=1}^{N} y(k)u(k-j)\\ \psi_{uu}(j) &= \lim_{N\to\infty}\frac{1}{N}\sum_{k=1}^{N} u(k)u(k-j)\end{aligned} \quad , \tag{10}$$

where N is the number of input-output observations.

If Eq.(9) is multiplied by u(k+2-j), then time correlations on both sides yield,

$$\psi_{yu}(j) = \phi_{yu}(j-1)^T\mathbf{a} + \phi_{uu}(j-1-\mu)^T\mathbf{b} + \lim_{N\to\infty}\frac{1}{N}\sum_{k=1}^{N}\xi(k+2)u(k+2-j), \tag{11}$$

where $\mathbf{a}^T=[a_1 \quad a_2]$, $\mathbf{b}^T=[b_1 \quad b_2]$, $\phi_{yu}(j-1)^T=[\psi_{yu}(j-2) \ \psi_{yu}(j-1)]$ and $\phi_{uu}(j-1-\mu)^T=[\psi_{uu}(j-2-\mu) \ \psi_{uu}(j-1-\mu)]$.

Supposing that u and ξ are uncorrelated each other, we have,

$$\lim_{N\to\infty}\frac{1}{N}\sum_{k=1}^{N}\xi(k+2)u(k+2-j) = 0 \ . \tag{12}$$

For $j=1,2,\cdots,n,n+1,\cdots,2n$, Eq.(11) can be written as

$$\mathbf{N} = \mathbf{M}\mathbf{P}, \tag{13}$$

where $\mathbf{N}^T=[\psi_{yu}(1) \ \psi_{yu}(2) \ \cdots \ \psi_{yu}(n) \ \psi_{yu}(n+1) \ \cdots \ \psi_{yu}(2n)]$

$\mathbf{P}^T=[\mathbf{a}^T\mathbf{b}^T]$

$$\mathbf{M} = \begin{bmatrix} \phi_{yu}(0)^T & \phi_{uu}(-\mu)^T \\ \phi_{yu}(1)^T & \phi_{uu}(1-\mu)^T \\ \vdots & \vdots \\ \phi_{yu}(n)^T & \phi_{uu}(n-\mu)^T \\ \phi_{yu}(n+1)^T & \phi_{uu}(n+1-\mu)^T \\ \vdots & \vdots \\ \phi_{yu}(2n-1)^T & \phi_{uu}(2n-1-\mu)^T \end{bmatrix} .$$

The least-squares parameter estimates are given by[3]

$$\hat{P} = [M^T M]^{-1} M^T N \tag{14}$$

where $\hat{\cdot}$ denotes the estimated value. (Appendix B) Through the calculations of Eq.(14) based on the data of both the input u(k) and the output y(k) over a finite time interval, the unknown parameters a_1, a_2, b_1 and b_2 can be determined uniquely, which are composed of system parameters c_1, c_0, σ_1 and σ_0.

4. Analytical Results

As illustrating examples, the following experiments have been performed for the estimation of unknown system parameters, in the cases where the atmospheric temperatures are 9°C and 16°C. The width of hysterisis in the relay element was set as h=131mV, and the output of the heater was 18.3w at 9°C and 18.3w at 16°C. In the input-output measurements, u(t) and y(t) were discretized at the interval of 0.1s by the A/D converter. The number of data was n=2,000.

Using these measured data, the unknown parameters have been estimated according to the method described in Chapter 3. Figures 5 and 6 show the estimated results in the case where the atmospheric temperature is 9°C. The estimated values $\hat{a}_1$ and $\hat{a}_2$ are shown in Fig.5 and $\hat{b}_1'$ and $\hat{b}_2'$ in Fig.6, respectively. Here, $\hat{b}_1'$ and $\hat{b}_2'$ in Fig.6 are defined as

$$\hat{b}_1' = \hat{b}_1/G, \quad \hat{b}_2' = \hat{b}_2/G \ , \tag{15}$$

where G is the gain constant determined by both the amplifier and the sensor, which is obtained from Eq.(8).

From Figs.5 and 6, the estimates $\hat{a}_1$ and $\hat{a}_2$ show a very good convergence to a constant value, respectively. However, the estimates $\hat{b}_1'$ and $\hat{b}_2'$ do not necessarily show a good convergence, although they have the tendency to converge to a constant value, respectively. It can be considered that this result can be caused by the following reasons. That is, the atmospheric temperature could not be held constant precisely, the heater output was always fluctuating slightly by the action of feedforward controller and the number of measurement data was not extracted sufficiently, etc. In Figs.5 and 6, the broken lines are values obtained through the individual experimental studies as before.[1]

The estimated model parameters with the correlation-regression method are

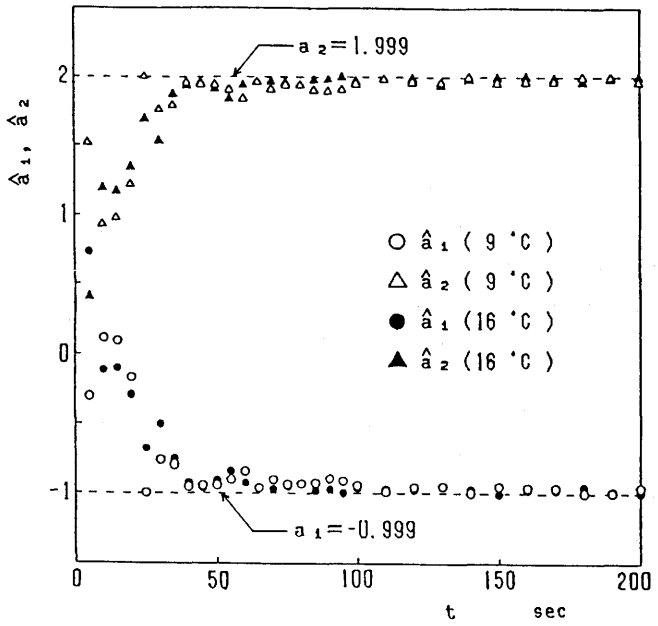

Fig.5 Estimates of a_1, a_2

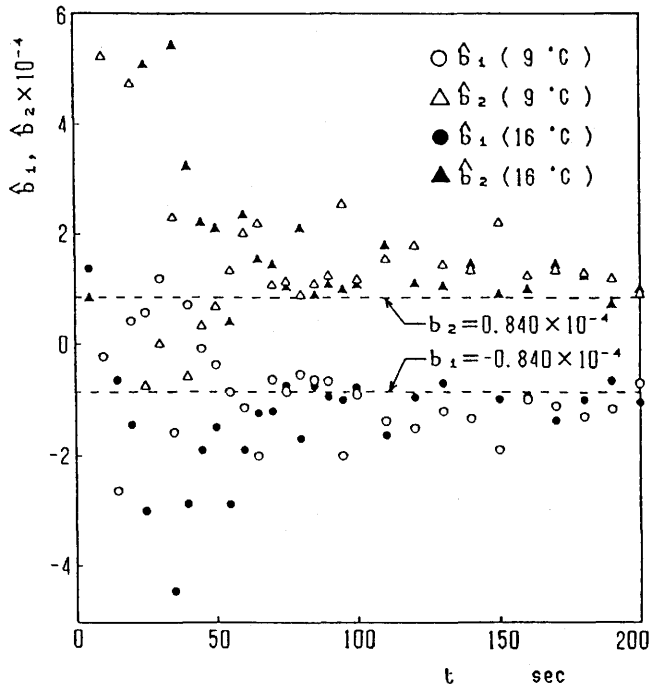

Fig.6 Estimates of b_1, b_2

$$\hat{a}_1 = -9.820\times10^{-1}, \quad \hat{a}_2 = 1.980, \quad \hat{b}_1' = -1.058\times10^{-4}$$

$$\hat{b}_2' = 1.201\times10^{-4}.$$

These values are the average of data in the time interval, $160s \leqq t \leqq 200s$. Using parameters $\hat{a}_1$, $\hat{a}_2$, $\hat{b}_1'$ and $\hat{b}_2'$ obtained here, the temperature characteristics of the stationary self-oscillation in the intermediate space are analyzed by the describing function method. As a result, it can be seen that the period of self-oscillation is 10.9s and the input amplitude to the relay element 2718 mV , from which the temperature amplitude in the intermediate space is 0.11°C. On the other hand, the experimental results show that the temperature deviation is 0.12°C and the period is 12.0s. Comparing with the theoretical results obtained by the parameter estimation, it follows that both the period and the temperature deviation agree with the experimental ones.

In the case where the atmospheric temperature is 16°C, the estimated parameters are,

$$\hat{a}_1 = -9.907\times10^{-1}, \quad \hat{a}_2 = 1.989, \quad \hat{b}_1' = -1.008\times10^{-4}$$

$$\hat{b}_2' = 1.091\times10^{-4}.$$

From these results, it follows that both the period and the temperature in the intermediate space agree with the experimental ones. These facts imply a good correspondence between the experiment of the practical device and the analysis of the system model established here.

5. Feedforward Control Experiments

In order to eliminate the shift of the center position in the stationary oscillation of the temperature due to the variation of the atmospheric temperature, the following two experiments have been carried out using the thermostatic device of Fig.1 equipped with the feedforward controller.

First, to ascertain the improvement of the characteristics by the addition of the feedforward controller, the experiment has been performed at the atmospheric temperature 19°C. The measurement results of both y(t) and u(t) are shown in Fig.7. Figure 7(a) shows the controlled state of the temperature in the intermediate space and (b) the output of the heater, in which at $t=t_f$ the feedforward controller begins to operate. From Fig.7, before the

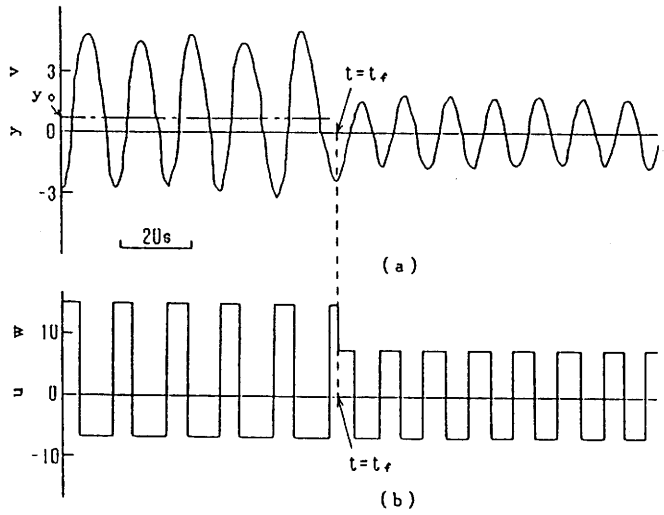

Fig.7 Feedforward Control Experiment I
(The State in Intermediate Space)

feedforward controller starts to work ($t \leq t_f$), the output of the heater becomes non-symmetric and also the steady state oscillation in the intermediate space non-symmetric. Then, the center position shifts only to y_0=1.1 v (0.04°C as the change of the temperature) from the reference one. However, it follows that, after the feedforward controller starts to work at $t=t_f$, the steady state oscillation in the intermediate space becomes symmetric and then the shift of the center position may be eliminated. Furthermore, in this experiment, the amplitude of the temperature in the intermediate space may be reduced from 0.15°C to 0.08°C due to the addition of the feedforward controller. Consequently, it is seen that the control accuracy can be improved by the feedforward controller.

Next, we examine the controlled temperature in the intermediate space in the case where the ambient temperature is slowly changed from 9°C to 19°C, under the condition that the feedforward controller is operating. Figure 8 shows the sample behaviors of y(t) and u(t) in both cases; (a) after beginning and (b) after 13 min.. As a result, even if the atmospheric temperature changes, the shift of the center position in the steady state oscillation can not be admitted in the intermediate space, as shown in Fig.8. Therefore, it is ascertained that the feedforward controller could operate

efficiently in this experiment. The average values of the temperature amplitude and period in the intermediate space are 0.12°C and 12.0s for the case that the atmospheric temperature changes from 9.5°C to 10.5°C; 0.08°C and 12.0s for the change from 14.5°C to 15.0°C; 0.07°C and 12.0s for the change from 19.5°C to 19.8°C, respectively. Accordingly, these results satisfy sufficiently the control accuracy for the thermostatic container. However, since it is, at present, difficult to measure precisely the amplitude of the temperature in the inner space, we could not give the positive evidence of the experimental results.

6. Conclusions

For a double-walled thermostatic container made on trial, which is one of the most important elements in the measuring device of barometric difference, the system identification from input-output measurements has been developed and the state of the temperature in the container clarified from both theoretical and experimental viewpoints. Furthermore, in order to eliminate the effect to the control accuracy of the temperature both in the intermediate and inner

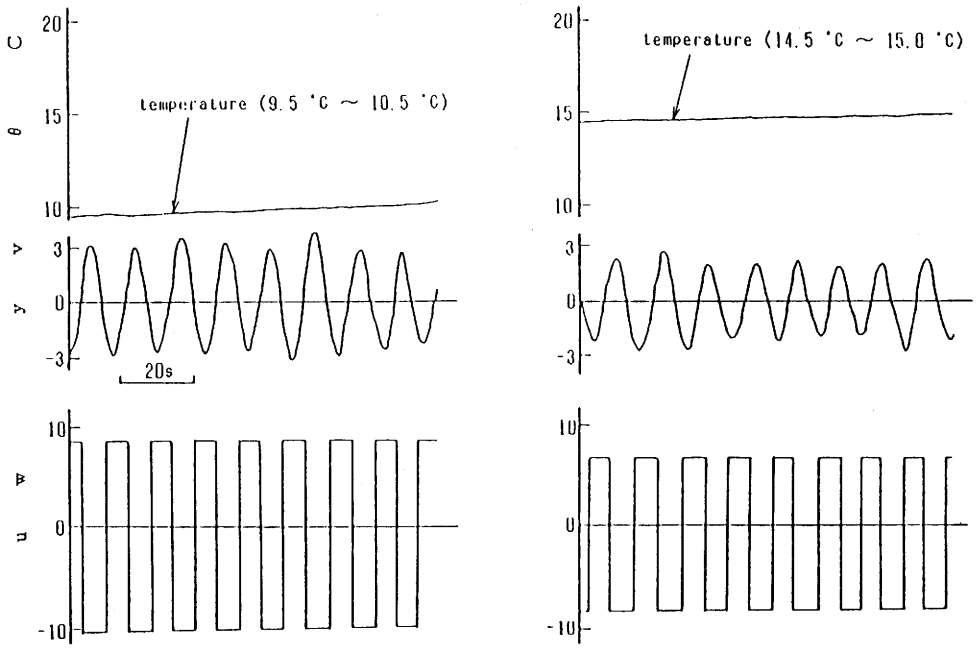

(a) after beginning (b) after 13 min.

Fig.8 Feedforward Control Experiment II

spaces by the variation of the atmospheric temperature, a feedforward controller has been implemented to regulate the sample temperature and the efficiency ascertained through the experiment. The results obtained above can be summarized as follows.

(1) The unknown parameters of a bilinear control system with respect to the thermostatic container has been estimated using the least-squares and the correlation-regression algorithms. The theoretical results, obtained through the estimated parameters, with respect to the temperature amplitude and period in the intermediate space, have shown the good consistency compared with the experimental ones. From this result, it has been shown that the state of the temperature regulation can be estimated precisely both in the intermediate and inner spaces.

(2) Though the steady state oscillation of the temperature in the intermediate space becomes non-symmetric due to the variation of the atmospheric temperature, the shift of the center position in the steady-state oscillation can be eliminated by the addition of a feedforward controller. From this result, the effect of the atmospheric temperature in the inner space can be taken away and the temperature regulation may be achieved with high accuracy.

(3) Using the temperature amplitude in the intermediate space obtained above, the temperature amplitude in the inner space can be estimated to be about 1×10^{-4}°C to 2×10^{-4}°C.

From described above, it has been shown that the estimation algorithm applied here has been effective to a simulation model of a double-walled thermostatic container and also the addition of the feedforward controller has been successfully applied for the temperature regulation of the container.

References

(1) T.Asakura et al., Trans. of JSME, 50-458, 2614(1984)

(2) T.Asakura et al., Mem. Fac. Eng., FUKUI UNIV., 34-1, 91(1986)

(3) Baheti,R.S., et al., IEEE Trans. Automatic Contr., AC-25, No.6, 1141(1980)

(4) Iserman,R. and Bauer,U., Trans. ASME, J.Dynamic Syst., Meas., Contr., 96-4, 426(1974)

[Appendix A] Derivation of Eq.(9).

From Eq.(6), it follows that

$$x_1(k+1) = \phi_{11}x_1(k) + \phi_{12}x_2(k) + D_1u(k) + F_1w(k) \qquad (A1)$$

$$x_2(k+1) = \phi_{21}x_1(k) + \phi_{22}x_2(k) + D_2u(k) + F_2w(k). \quad (A2)$$

Using Eqs.(A1) and (A2), we obtain

$$\begin{aligned} x_1(k+2) = {} & (\phi_{11} + \phi_{22})x_1(k+1) \\ & + (\phi_{12}\phi_{21} - \phi_{11}\phi_{22})x_1(k) + D_1u(k+1) \\ & + (\phi_{12}D_2 - \phi_{22}D_1)u(k) + F_1w(k+1) \\ & + (\phi_{12}F_2 - \phi_{22}F_1)w(k) . \end{aligned} \quad (A3)$$

From Eq.(7), it becomes,

$$y(k) = Gx_1(k-\mu) + v(k). \quad (A4)$$

Using Eqs.(A3) and (A4), we obtain

$$\begin{aligned} y(k+2) = {} & (\phi_{11} + \phi_{22})y(k+1) \\ & +(\phi_{12}\phi_{21} - \phi_{11}\phi_{22})y(k) + GD_1u(k+1-\mu) \\ & +G(\phi_{12}D_2 - \phi_{22}D_1)u(k-\mu) + GF_1w(k+1-\mu) \\ & +G(\phi_{12}F_2 - \phi_{22}F_1)w(k-\mu) + v(k+2) \\ & -(\phi_{11} + \phi_{22})v(k+1) - (\phi_{12}\phi_{21} - \phi_{11}\phi_{22})v(k) \end{aligned} \quad (A5)$$

In Eq.(A5), Letting be

$$\phi_{11} + \phi_{22} = a_2;\ \phi_{12}\phi_{21} - \phi_{11}\phi_{22} = a_1;\ GD_1 = b_2;\ G(\phi_{12}D_2 - \phi_{22}D_1) = b_1;\ GF_1w(k+1-\mu) + G(\phi_{12}F_2 - \phi_{22}F_1)w(k-\mu) + v(k+2) - (\phi_{11} + \phi_{22}) \times v(k+1) - (\phi_{12}\phi_{21} - \phi_{11}\phi_{22})v(k) = \xi(k+2),$$

we obtain Eq.(9).

[Appendix B] Derivation of Eq.(14)

Let the criterion be chosen as to minimize the loss function,

$$V = \sum_{k=0}^{2n} e^2(k) = \mathbf{e}^T\mathbf{e} . \quad (B1)$$

An Equation error is defined,

$$\mathbf{e} = \hat{\mathbf{N}} - \hat{\mathbf{N}}_{2n} , \quad (B2)$$

which is an error between the new observation $\hat{\phi}_{uy}$ and its prediction by the model. The minimum of loss function (B1) is found through the calculation of

$$dV / d\mathbf{P} = 0, \quad (B3)$$

with respect to the parameters P. Using Eq.(13) and (B2), we obtain the least squares parameter estimate Eq.(14). This estimate is consistent in mean square sense.